Multilevel Upscaling through Variational Coarsening

Scott P. MacLachlan

Department of Applied Mathematics, University of Colorado
Boulder, CO, 80309

J. David Moulton

Mathematical Modeling and Analysis Group, Los Alamos National Laboratory
Los Alamos, NM, 87545

Abstract.
A new efficient multilevel upscaling procedure for single-phase saturated flow in porous media is presented. While traditional approaches to this problem have focused on the computation of an upscaled hydraulic conductivity, here the coarse-scale model is created explicitly from the fine-scale model through the application of operator-induced variational coarsening. This technique, which originated with robust multigrid solvers, has been shown to accurately capture the influence of fine-scale heterogeneous structure over the complete hierarchy of coarse-scale models that it generates. Moreover, implicit in this hierarchy is the construction of interpolation operators that provide a natural and complete multiscale basis for the fine-scale problem. Thus, this new multilevel upscaling methodology is similar to the Multiscale Finite Element Method (MSFEM) and, indeed, it attains similar accuracy in computations of the fine-scale hydraulic head and coarse-scale normal flux on a variety of problems; yet it is an order of magnitude faster on the examples considered here.

Citation: MacLachlan, S. P., and J. D. Moulton (2006), Multilevel upscaling through variational coarsening, *Water Resour. Res.*, *42*, W02418, doi:10.1029/2005WR003940.

1. Introduction

Although the increasing power of modern computer hardware enables effective simulation of many single-scale and single-component systems, there exist fundamental mathematical and algorithmic challenges in the effective simulation of multi-scale and multi-component systems. In particular, a critical underlying problem in the numerical modeling of flow in porous media is the need to resolve the multiscale structure of the subsurface environment. For example, the length scales observed in sedimentary laminae range from the millimeter scale upward, while the simulation domain may be on the order of several kilometers. As a result, fully resolved simulations are computationally intractable, yet the fine-scale variations of the model parameters (e.g., structure and orientation of laminae) significantly affect the properties of the solution at all scales.

Many methods have been proposed to address the complication of fine-scale variation in the material parameters of a porous medium. Although an important aspect of this multifaceted problem is the uncertain specification of the true fine-scale structure, which is often treated stochastically, here we focus on the deterministic case in which a fine-scale description of the medium is assumed a priori. If certain structural information of the medium is known, then it may be possible to derive a useful coarse-scale model using simple averages. In the case of mean uniform flow, for example, the effective permeability of a medium is bounded between the harmonic and arithmetic averages of the fine-scale permeability, as shown in *Cardwell and Parsons* [1945], along with conditions on the media and flows where these bounds are achieved. The geometric average (*Warren and Price* [1961]) and certain power averages (*Desbarats* [1992a]) provide reliable approximations of the effective permeability if the fine-scale variation in the permeability field satisfies certain conditions. Similarly, in the case of nonuniform flow, *Desbarats* [1992b] demonstrates that a weighted geometric average provides accurate effective transmissivities for low to moderate variances of the log-transmissivity field. To expand the applicability of simple averages fur-

ther, *Ebrahimi and Sahimi* [2002] developed wavelet transformation techniques that guide spatially adaptive averaging to generate a compressed representation of the conductivity field. The thresholding parameters in this approach effectively prevent averaging across strongly discontinuous interfaces, and hence, its balance of accuracy and efficiency depends strongly on the fine-scale structural properties of porous medium. Ultimately, however, the underlying fundamental limitation of these approaches is that none of these simple averages accurately capture the coarse-scale dynamics of an arbitrary medium under arbitrary flow conditions. In more complex problems, such as transient multiphase flow, coarse-scale models cannot be completely decoupled from the fine-scale dynamics.

The purpose of this paper is to introduce a new multilevel upscaling algorithm, based on variational principles, that accurately and efficiently captures the effects of a multiscale medium. The fine-scale permeability is not explicitly averaged, neither through a simple average chosen a priori, nor through the solution of local problems as in *Durlofsky* [1991]. In fact, no solution of any fine-scale problems is required by the method. Instead, variational multigrid principles (cf. *Bank et al.* [1985]) are used to construct a self-consistent hierarchy of coarse-scale models directly from the given fine-scale model. Moreover, the solution of a coarse-scale model yields information at more than just that scale, as important finer-scale information is preserved through the hierarchy.

This multilevel approach yields more information than equivalent or effective permeabilities defined over coarse-scale blocks, regardless of whether the coarse-scale permeabilities are calculated using simple averages, as above, or with more sophisticated techniques such as the upscaling of *Durlofsky* [1991] and *He et al.* [2002] that relies on the solution of local fine-scale problems. These techniques, referred to as Laplacian methods in the review by *Wen and Gómez-Hernández* [1996], are more accurate, in general, than simple averages. However, the linear scaling of multigrid iterative solvers for elliptic problems (*Braess and Hackbusch* [1983]) implies that solving the necessary local fine-scale problems is asymptotically no less expensive than solving the global fine-scale problem, unless there is some periodic behavior in the fine-scale permeability that can be exploited. Moreover, such an approach yields only a coarse-scale representation of the flow properties, potentially missing important dynamics necessary to accurately simulate multiphase flows. Comparisons with the Laplacian upscaling of *Durlofsky* [1991] have shown that the multilevel upscaling proposed here is significantly more accurate, as well as computationally more efficient (*MacLachlan* [2004]).

In this paper, we present a comparison with the multiscale finite element method (MSFEM), which was demonstrated in *Hou and Wu* [1997] and analyzed by *Hou et al.* [1999]. This method is similar in both approach and accuracy to the multilevel upscaling ideology considered here. In addition, its application to the simulation of flows in heterogeneous porous media is being actively pursued by the community (*Ye et al.* [2004]). In the MSFEM, multiscale dynamics are captured through the computation of local, low-energy basis functions used to reduce the problem to a chosen coarse scale. The explicit construction of these basis functions accurately represents fine-scale dynamics of the flow; however, this comes at the cost of solution of a set of local fine-scale problems, resulting in an overall cost similar to that of solving the global fine-scale model.

The multilevel upscaling algorithm developed here attains accuracy comparable to the MSFEM approach, but at a significantly lower cost. Both approaches are variational, representing the low-energy components of the model on coarse scales, preserving the minimization properties of the fine-scale finite element discretization. The recursive approach of a multigrid framework, however, allows explicit coarsening of the fine-scale problem without performing any local solves. Instead, physical heuristics are used to identify local characteristics of low-energy error and represent such components on coarser scales.

This paper proceeds as follows. Section 2 introduces the continuum-scale mathematical model of saturated, single-phase flow through porous media and the finite-element discretization that we consider here. In Section 2.1, we discuss the details of variational multigrid, followed by a description of the multilevel upscaling algorithm in Section 2.2. A periodic model problem is discussed in Section 3, where the intuition gained from a simple medium is used to clarify the approach. More complex media are considered in Section 4. Conclusions are presented in Section 5.

2. Background and Method

We consider two-dimensional single-phase saturated flow through a porous medium whose hydraulic conductivity, $\mathcal{K}(\boldsymbol{x})$, is specified on a fine-scale over the domain of interest, Ω. This flow may be modeled at the continuum scale using Darcy's law and conservation of mass,

$$\boldsymbol{q}(\boldsymbol{x}) = -\mathcal{K}(\boldsymbol{x})\nabla h(\boldsymbol{x}), \tag{1}$$

$$\nabla \cdot \boldsymbol{q}(\boldsymbol{x}) = Q(\boldsymbol{x}), \tag{2}$$

for all $\boldsymbol{x} \in \Omega$. Here, $h(\boldsymbol{x})$ is the hydraulic head, $\boldsymbol{q}(\boldsymbol{x})$ is the Darcy flux, and $Q(\boldsymbol{x})$ represents any external sources or sinks of fluid. The conductivity, $\mathcal{K}(\boldsymbol{x})$, is a positive scalar or a positive definite tensor that is assumed to be piecewise smooth with jump discontinuities at interfaces. We consider

problems with a combination of no-flow boundary conditions (homogeneous Neumann),

$$\boldsymbol{q}(\boldsymbol{x}) \cdot \mathbf{n} = 0\,, \quad \forall \boldsymbol{x} \in \Gamma_{\mathrm{N}}\,, \tag{3}$$

and prescribed hydraulic head (Dirichlet),

$$h(\boldsymbol{x}) = h_D(\boldsymbol{x})\,, \quad \forall \boldsymbol{x} \in \Gamma_{\mathrm{D}}\,, \tag{4}$$

where $h_D(\boldsymbol{x})$ is a smooth function along the boundary.

In the following discussion, we work with this model in its second order form,

$$-\nabla \cdot [\mathcal{K}(\boldsymbol{x})\nabla h] = Q(\boldsymbol{x}), \tag{5}$$

from which a fine-scale discrete model may be obtained with bilinear finite elements on a uniform rectangular mesh that resolves the variation in $\mathcal{K}(\boldsymbol{x})$. Specifically, in the standard Galerkin finite-element formulation, we write

$$h(\boldsymbol{x}) = \sum_{i=1}^{N} h_i \phi_i(\boldsymbol{x}), \tag{6}$$

where $\{\phi_i(\boldsymbol{x})\}$ are the nodal basis functions associated with the rectangular mesh of N nodes. Substitution of (6) into the weak form of (5) results in a discrete problem that may be expressed as a sparse linear system of equations,

$$A\mathbf{h} = \mathbf{Q}, \tag{7}$$

where $\mathbf{h} = (h_1, \ldots, h_N)^T$ and $\mathbf{Q} = (Q_1, \ldots, Q_N)^T$. The elements of the large, sparse $N \times N$ matrix, A, are given by

$$a_{ji} = \int_{\Omega} (\mathcal{K}(\boldsymbol{x})\nabla\phi_i(\boldsymbol{x})) \cdot \nabla\phi_j(\boldsymbol{x}) d\Omega. \tag{8}$$

Note that since $\mathcal{K}(\boldsymbol{x})$ is everywhere symmetric and positive-definite, so is A.

2.1. Variational Multigrid Coarsening

A fully resolved mesoscale simulation of flow through strongly heterogeneous media is likely to remain intractable for some time. Thus, an approach is needed to accurately and efficiently capture the influence of fine-scale structure over a hierarchy of coarse-scale models. Many key ingredients of this hierarchy are found in existing multilevel iterative algorithms, such as multigrid. Specifically, these methods achieve their efficiency through the recursive use of successively coarser discrete problems (i.e., a hierarchy of coarse-scale discrete models), in conjunction with a complementary smoothing iteration. In fact, these methods have been shown to scale optimally with N (i.e., solution cost grows only linearly with N) for a broad class of problems, suggesting that scale interaction is well characterized by this approach. Of particular interest here is a class of robust *black box* methods that use the fine-scale discrete model to construct, through a variational principle, the successively coarser coarse-scale operators. In this paper, we use the fundamental components of the *black box multigrid* (BoxMG) algorithm (*Dendy* [1982]) in our multilevel upscaling approach.

An excellent introduction to multigrid methods is given by *Briggs et al.* [2000]. Here, it is sufficient to highlight the key steps in the multigrid solution of Equation (7), which are shown schematically in Figure 1 and described as follows:

- the residual on a particular grid is smoothed (so that it can be well approximated on a coarser grid)
- the residual is then *restricted* to the coarser grid
- repeat recursively until the coarsest grid is reached
- solve for the error on the coarsest grid
- *interpolate* a correction to the next finer grid and add to current approximation
- compute and then smooth the new residual
- repeat to undo the recursive coarsening

We note that the residual of Equation (7), for the j^{th} approximation of the hydraulic head, $\mathbf{h}^j$, is simply $\mathbf{r}^j = \mathbf{Q} - A\mathbf{h}^j$.

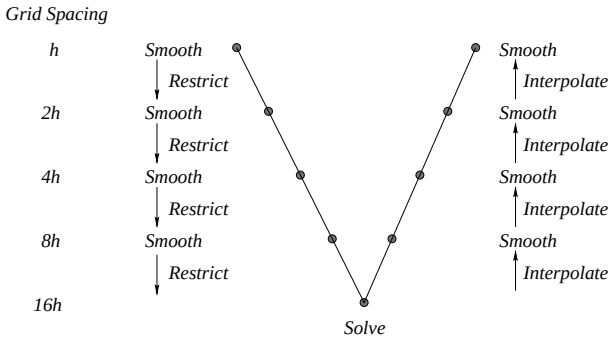

Figure 1. Schematic of a V-cycle multigrid iteration. On each level, the residual is reduced by a smoothing iteration, then transferred recursively to the next coarser scale. The correction from the coarsest scale is computed directly. After the recursive call, the correction is interpolated and added to the current approximation on that scale, the new residual is then computed and smoothed.

From this description, it is apparent that the efficiency of a multigrid algorithm is tightly coupled to the performance of the smoother (although this component is beyond the scope of this discussion). Smoothing on coarse levels requires a representation of the fine-scale operator on these levels; we

utilize these operators in the upscaling algorithm that follows and, thus, focus here on their specification.

Consider a nested sequence of uniform rectangular meshes labeled $k = 1, \ldots, k_f$, where $k = 1$ denotes the coarsest grid and $k = k_f$ denotes the finest grid. A critical aspect of creating a multigrid algorithm is the hiearchy of coarse-grid operators, denoted A_k. In addition, we need to define the intergrid transfer operators: the interpolation operator, denoted P_{k-1}^k, interpolates functions from grid $(k-1)$ to grid k; the restriction operator, denoted R_k^{k-1}, restricts a function from grid $k-1$ to grid k. Variational coarsening offers one means of defining A_{k-1} in terms of A_k, R_k^{k-1}, and P_{k-1}^k. In particular, restating the discrete linear system as an equivalent minimization problem, and then restricting this minimization to the range of interpolation yields (cf. *Nicolaides* [1979], *Brandt* [1984]),

$$A_{k-1} = \left(P_{k-1}^k\right)^* A_k P_{k-1}^k \,, \tag{9}$$

and, thus, we take the restriction to be the adjoint of interpolation, $R_k^{k-1} = \left(P_{k-1}^k\right)^*$.

Finally, to complete the specification of a variational coarsening algorithm, we must define the interpolation operator. In fact, the choice of the interpolation operator is critical to the robustness and efficiency of the resulting multigrid algorithm. For example, a naive choice such as bilinear interpolation erroneously assumes that the gradient of the hydraulic head is continuous and generates a coarse-scale model in which the upscaled hydraulic conductivity is simply an arithmetic average of the fine-scale conductivity. Thus, it is not surprising that bilinear interpolation leads to a fragile multigrid algorithm that is not suitable for strongly heterogeneous media. Instead, a significantly better approach is to use entries in the fine-scale discrete operator to define an interpolation that preserves certain fundamental properties of the solution. This technique was dubbed operator-induced interpolation by *Dendy* [1982]. The BoxMG interpolation scheme considered here was shown by *Moulton et al.* [1998] to approximately enforce the continuity of the normal component of the Darcy flux across interfaces.

2.2. The Multilevel Upscaling (MLUPS) algorithm

Given a fine-scale model, A_{k_f}, the variational coarsening presented in Section 2.1 generates a complete hierarchy of interpolation operators, P_{k-1}^k, and coarse-scale models, A_k. Using this variational coarsening procedure, the coefficients of interpolation and the coarse-scale models depend only on the given fine-scale model, A_{k_f}. When the coarsening is consistent with physical or mathematical properties of the model, these useful properties are typically preserved in the coarse-scale models of the hierarchy. For example, variational coarsening preserves the symmetry and definiteness of the fine-scale operator, A_{k_f}, and, at each level, the resulting correction minimizes the error in the range of the interpolation (cf. *Nicolaides* [1979], *Brandt* [1984]). More importantly for upscaling applications, variational coarsening implicitly generates multiscale basis functions (*Grauschopf et al.* [1997]). To clarify this property, denote, on each scale k, the set of basis functions $\{\psi_j^k\}$, which we define recursively from the finest scale. On the scale of discretization, grid k_f, the basis functions are simply the bilinear basis functions used in Equation (6), $\psi_j^{k_f} = \phi_j$, for all fine-scale nodes j. Given an operator, A_k, on level k, generated by basis functions ψ_j^k,

$$\left(A_k\right)_{ij} = \int_\Omega \left\langle \mathcal{K}(\boldsymbol{x}) \nabla \psi_j^k, \nabla \psi_i^k \right\rangle d\Omega, \tag{10}$$

denote the elements of the interpolation as $\left(P_{k-1}^k\right)_{ij} = p_{ij}^k$, such that substitution in (9) gives

$$\begin{aligned} \left(A_{k-1}\right)_{ij} &= \sum_{l,m} p_{li}^k \, p_{mj}^k \int_\Omega \langle K(x) \nabla \psi_m^k, \nabla \psi_l^k \rangle d\Omega \\ &= \int_\Omega \left\langle K(x) \nabla \Big(\sum_m p_{mj}^k \, \psi_m^k \Big), \nabla \Big(\sum_l p_{li}^k \, \psi_l^k \Big) \right\rangle d\Omega. \end{aligned} \tag{11}$$

Hence, if we define the new multiscale basis functions on level $k-1$ as

$$\psi_j^{k-1} = \sum_m p_{mj}^k \, \psi_m^k \,, \tag{12}$$

we may write the discrete coarse-grid operator in the form

$$\left(A_{k-1}\right)_{ij} = \int_\Omega \left(\mathcal{K}(\mathbf{x}) \nabla \psi_j^{k-1}, \nabla \psi_i^{k-1} \right) d\Omega \,. \tag{13}$$

Therefore, interpolation provides not only mappings between grid function spaces but may also be viewed as part of the discretization on coarse grids. It is in this way that the variational definition of the coarse-grid operator may be viewed as a discrete method for generating a hierarchy of coarse-scale discrete models that accurately capture the influence of the fine-scale heterogeneous structure.

Our new multilevel upscaling (MLUPS) algorithm uses the components of the black box multigrid algorithm (or BoxMG, cf. *Dendy* [1982]) in the following way:

1. Create a conforming bilinear discretization of Eq. (5) on the finest grid, imposing homogeneous Neumann boundary conditions on the entire domain.
2. Construct the multilevel basis functions and the variational hierarchy of coarse-scale models:

- use operator-induced interpolation from BoxMG to define the interpolation operators, P_{k-1}^{k}.
- use the variational coarsening given in Eq. (9) to define the coarse-scale operators, A_{k-1}.

3. Select a coarse-scale, $k = k_c$, on which to define the coarse-scale approximation of Equation (7). Then, restrict the given fine-scale boundary conditions and source to level k_c, to define this coarse-scale model, $A_{k_c}\mathbf{h}_{k_c} = \mathbf{Q}_{k_c}$.
4. Use BoxMG to solve the discrete coarse-scale model on level k_c.
5. Interpolate the coarse-scale solution from level k_c to the finest level, k_f, using the multiscale basis functions defined by Eq. (12).

It is important to note that the fine-scale discretization matrix in Step 1, A_{k_f}, is created with full homogeneous Neumann boundary conditions. These are the natural boundary conditions for the weak form of this flow model, and they generate a fine-scale discrete model that contains full fine-scale conductivity information. In turn, this leads naturally to a complete coarse-scale model that offers the flexibility of imposing boundary conditions directly on that scale. In fact, the actual boundary conditions for the flow of interest are coarsened separately (although consistently with the Neumann case) and applied on the chosen coarse scale.

3. Periodic Media

We first apply the MLUPS algorithm (Section 2.2) to a model problem with a two-scale periodic variation in the hydraulic conductivity. Specifically, we consider a structured pattern of square inclusions of a high conductivity medium in a homogeneous background, as depicted on the left of Figure 2. The conductivity is constructed by a four by four tiling of the unit cell shown on the right of Figure 2, where the $\mathcal{K}(\boldsymbol{x}) = 1000$ inside the dark region and $\mathcal{K}(\boldsymbol{x}) = 1$ in the background medium. This regular pattern provides an ideal setting to develop intuition into the MLUPS approach as the resulting multiscale basis functions clearly display the influence of this structure on the flow. Results for randomly generated anisotropic heterogeneous media are presented in the following section.

One approach to visualizing the MLUPS multiscale basis functions is to associate each basis function with a coarse-grid node on each level of the multigrid hierarchy. In this case, as we traverse the hierarchy to coarser scales, the support of a basis function grows and, hence, its shape captures an increasing region of fine-scale structure. In our current work with BoxMG, we use standard coarsening, which takes

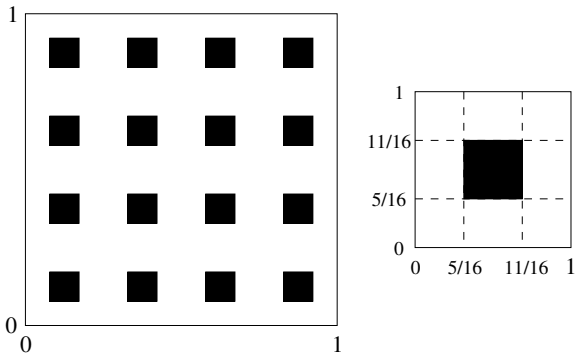

Figure 2. Periodic conductivity field. The field on the left is created by a 4×4 tiling of the unit cell at the right. $\mathcal{K} = 1000$ in the dark region, and $\mathcal{K} = 1$ in the light region.

half of the points in each coordinate direction at each level. Thus, the number of points is reduced by a factor of four on each level and, moreover, the support of the multiscale basis function grows in area by a factor of four with each level.

However, this approach is not particularly informative for this model problem because it takes too many levels for the support of the coarse-scale basis functions to cover interesting features of the conductivity field. Instead, we examine how the information in the multigrid interpolation operators compounds from the coarsest scales up to the finest. Figure 3 shows this development on the coarse scales, where we see the evolution of the basis function centered at $(\frac{1}{2}, \frac{1}{2})$ from the bilinear basis function normally used on any scale to the effective MLUPS basis function for these scales in Figure 4. The support of the basis function does not grow relative to the problem domain; rather, as information is added from each interpolation operator, a better description of the behavior of the basis function over its fixed support is obtained. Once this information is incorporated on a scale where variations in $\mathcal{K}(\boldsymbol{x})$ are well represented, the basis function on that scale also represents the desired fine-scale behavior.

The MLUPS basis function exhibits many features appropriate for this flow. In the regions where $\mathcal{K}(\boldsymbol{x})$ is large, we expect small gradients of head relative to those in the background medium (since $\mathcal{K}\nabla h \cdot \mathbf{n}$ is constant across interfaces and we have a divergence free Darcy flux, locally as well as globally) ; the basis function reflects this with plateaus in its surface. Outside these regions, we do not know, a priori, what to expect of the hydraulic head for a general flow situation, and so bilinear tendencies are retained to best fit general heads on the coarse scale.

To demonstrate the accuracy of the MLUPS basis functions, we consider Equation (5), subject to no-flow boundary

conditions on the top and bottom edges, with heads $h = 1$ along $x = 0$ and $h = 0$ along $x = 1$. We then compute errors in both the hydraulic head and the average normal flux relative to the fine-scale *true* solution obtained on a 256×256 mesh with standard bilinear finite elements. Specifically, the errors in the head are measured in the discrete vector norms

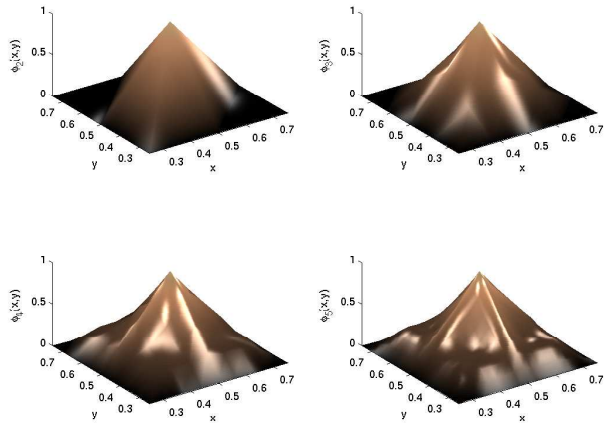

Figure 3. Coarse-scale basis functions for the periodic problem centered at $(\frac{1}{2}, \frac{1}{2})$ and viewed on the coarse 4×4 mesh. The level index $k = k_c = 2$ in the upper left, and increases by column and then row. The support of the basis function does not change, but fine-scale information is added to the bilinear basis function on level k_c through the recursive application of the multilevel basis definition in Equation (12).

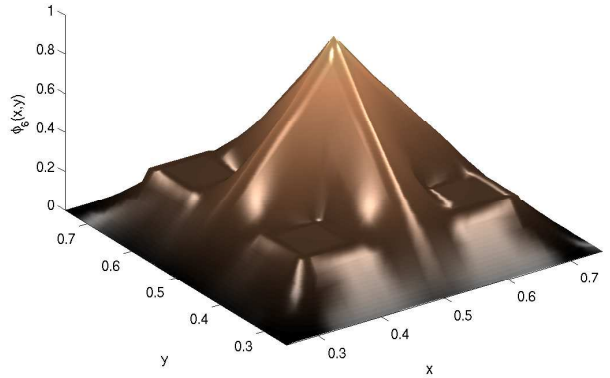

Figure 4. Fine-scale basis function, $k = k_f = 6$ for the periodic problem centered at $(\frac{1}{2}, \frac{1}{2})$ with support on the coarse 4×4 mesh obtained from the recursive application of Equation (12). Here the influence of the periodic structure on the flow is clearly captured in the multilevel basis function.

approximating $L_2(\Omega)$,

$$\|e(h)\|_2 = \left(\frac{1}{N} \sum_{i=1}^{N} e(h)_i^2 \right)^{\frac{1}{2}}, \tag{14}$$

where N is the number of nodes on the fine mesh, and approximating $L_\infty(\Omega)$,

$$\|e(h)\|_\infty = \max_i |e(h)_i| . \tag{15}$$

Similarly, to quantify the accuracy of the computed Darcy flux we consider the average flux through the domain,

$$\boldsymbol{q}_x = \int_0^1 (\boldsymbol{q} \cdot \hat{\boldsymbol{x}}) dy = \int_0^1 \left[-\mathcal{K}(x,y) \nabla h(x,y) \cdot \left(\begin{smallmatrix} 1 \\ 0 \end{smallmatrix} \right) \right] dy, \tag{16}$$

and define the corresponding discrete vector norms approximating $L_2([0,1])$,

$$\|e(\boldsymbol{q}_x)\|_2 = \left(\frac{1}{N_x} \sum_{i=1}^{N_x} e(\boldsymbol{q}_x)_i^2 \right)^{\frac{1}{2}}, \tag{17}$$

where N_x is the number of nodes in the x-direction on the fine mesh, and approximating $L_\infty([0,1])$,

$$\|e(\boldsymbol{q}_x)\|_\infty = \max_i |e(\boldsymbol{q}_x)_i|. \tag{18}$$

These results are summarized in Table 1, where the computational fine-scale ranges from 64×64 elements (a standard bilinear discretization) to 8×8 MLUPS elements. Note that as the number of degrees of freedom on the computational scale decreases, we see increasing L_2 errors in both head and average flux. The L_∞ error in pressure, however, remains relatively constant. This max-norm error is attained along lines of constant y, midway between the high-conductivity inclusions, where the MLUPS method tends to undershoot the exact solution producing a small cusp in the y-direction instead of the smooth but rapidly varying profile of the fine-scale conductivity.

Table 1. Errors in computed head and average normal flux for model problem with periodic conductivity.

Grid	$\|e(h)\|_2$	$\|e(h)\|_\infty$	$\|e(\boldsymbol{q}_x)\|_2$
64^2	4.29×10^{-4}	4.54×10^{-3}	7.45×10^{-3}
32^2	5.52×10^{-4}	3.92×10^{-3}	2.29×10^{-2}
16^2	1.04×10^{-3}	4.02×10^{-3}	7.16×10^{-2}
8^2	1.54×10^{-3}	6.62×10^{-3}	3.67×10^{-2}

To better understand this performance, recall that we discretized Equation (5) with finite elements, and, specifically,

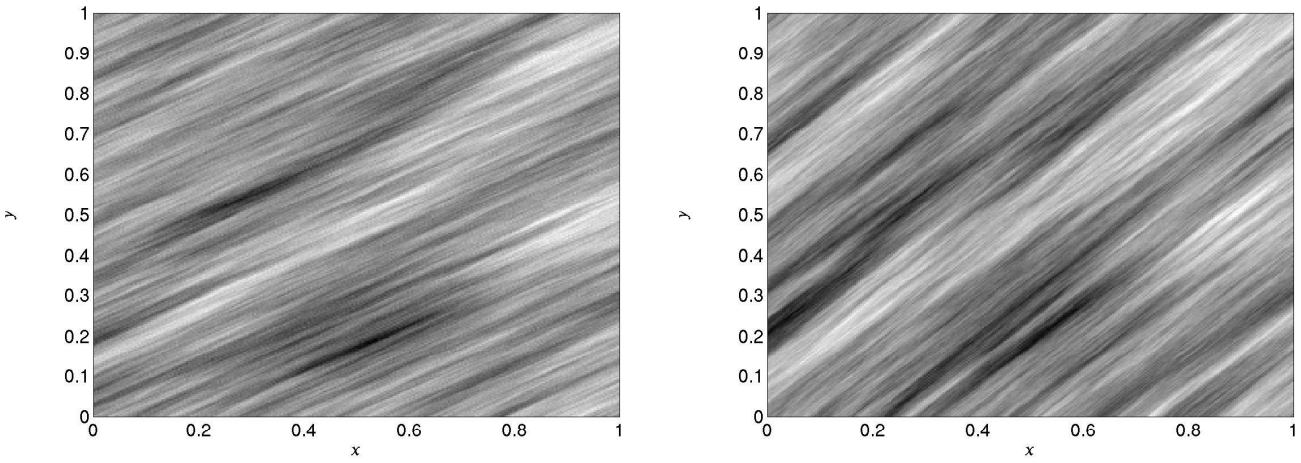

Figure 5. Conductivity field for 30° axis of anisotropy (left) and 45° (right). Fields were generated using the GSLIB software package, for a log-normal distribution with variance 4 with correlation lengths of 0.8 along the axis of anisotropy and 0.04 orthogonal to this axis. Conductivities range from approximately 10^{-3} (white) to 10^3 (black).

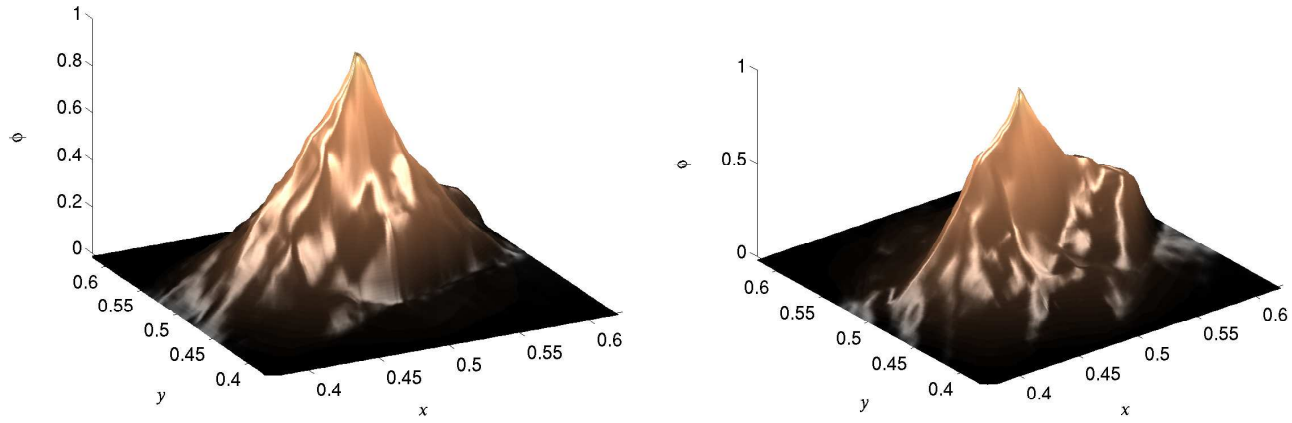

Figure 6. MLUPS basis function for the node $(\frac{1}{2}, \frac{1}{2})$ on an 8×8 grid for 30° axis of anisotropy (left) and 45° (right). Note that the axes of anisotropy are clearly reflected in the ridges displayed by both basis functions, and that they reflect expected features of the flow, changing quickly when $\mathcal{K}$ is small, and slowly when $\mathcal{K}$ is large.

that the solution of the computational fine-scale equations is the same as that of the minimization problem,

$$h = \underset{\tilde{h}\in\mathcal{V}}{\operatorname{argmin}} \iint \left(\frac{1}{2}(\mathcal{K}\nabla\tilde{h}) \cdot \nabla\tilde{h} - Q\tilde{h} \right) d\boldsymbol{x}.$$

The MLUPS method may be viewed as picking a subset of the space, $\mathcal{V}$, over which to perform the minimization. The natural weighting in the minimization functional, however, emphasizes errors in the regions where $\mathcal{K}(\boldsymbol{x})$ is large and/or the gradient of the hydraulic head is large. In a sense, this forces MLUPS to choose basis functions that allow small errors in the head in the background medium so that it can match the head more accurately in the high conductivity regions. Such an approach is consistent with the fine-scale finite element discretization and the variational framework of the Galerkin Finite Element Method and is, thus, viewed as a feature of the method.

4. Anisotropic Heterogeneous Media

While the example in Section 3 is useful as an introduction to the MLUPS methodology, it does not represent typical conductivity fields for which coarse-scale models are needed. A more realistic representation may be obtained with a random field generator. Thus, in this section, we focus on realizations of heterogeneous layered media, and examine the effect of such layering on the performance of the MLUPS method. Specifically, we consider a series of problems in which the hydraulic conductivity, $\mathcal{K}(\boldsymbol{x})$, is generated using the GSLIB software package (*Deutsch and Jour-*

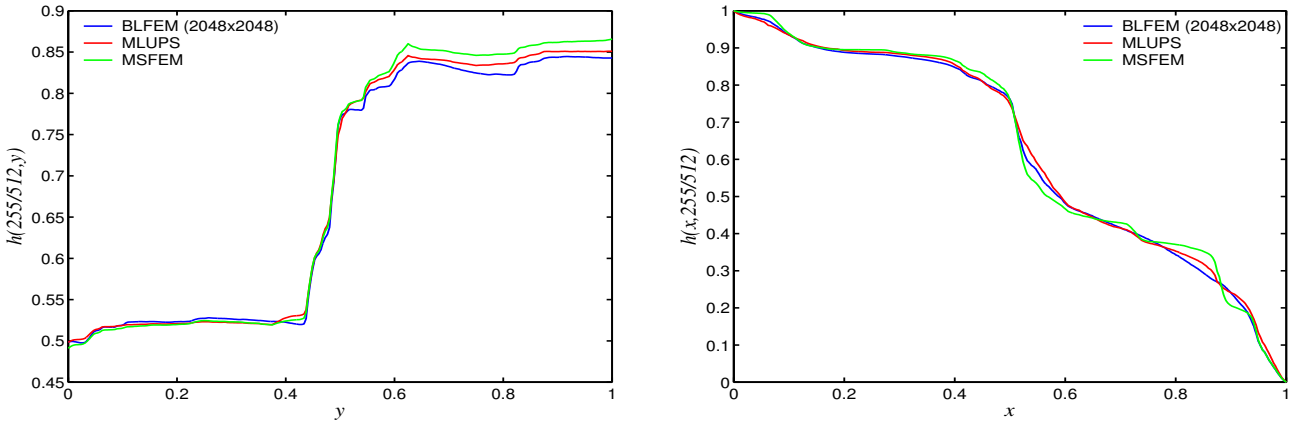

Figure 7. Cross-sections of the hydraulic head for fixed $x = \frac{255}{512}$ (left) and $y = \frac{255}{512}$ (right), generated by MLUPS and MSFEM upscaled to an 8×8 grid for the 30° axis of anisotropy, as in Figure 5. For comparison, the fine-scale hydraulic head was calculated on a 2048×2048 grid.

nel [1998]). The computational fine scale is selected as a 256×256 element grid and, on each element, the hydraulic conductivity is taken to be a constant. A principle axis of statistical anisotropy is selected between 0 and 90 degrees, relative to the positive x-axis, and a conductivity field is generated such that $\log_{10}(\mathcal{K}(\boldsymbol{x}))$ is normally distributed with mean zero and variance 4, with correlation lengths of 0.8 along the principle axis and 0.04 in the direction orthogonal to this axis.

Samples of these conductivity fields are shown in Figure 5, for the angles to the principle axis of 30° on the left and 45° on the right. The gray scale in these figures represents a range in conductivity from approximately 10^{-3} (white) to 10^3 (black). Notice the strong layering that results from the significant difference in the correlation lengths along and orthogonal to the chosen axis. The MLUPS basis functions for the node at $(\frac{1}{2}, \frac{1}{2})$ after upscaling by a factor of 32 in each direction are shown in Figure 6 for 30°, on the left, and 45°, on the right. These basis functions strongly reflect the fine-scale features of the conductivity. Most noticeable is the rotation in the features to match the angles of the layering in the conductivity, visible along the lower-right edges of the basis functions. Notice also how these basis functions strongly represent the expected behavior of the head for general flow conditions, with relatively small gradients in regions of large conductivity and relatively large changes in regions where the conductivity values are small.

Because of the similarity in approach of the two methods, we compare the results generated by the MLUPS method with the MSFEM of *Hou and Wu* [1997], and *Hou et al.* [1999]. The MSFEM method considers a given fine computational scale and explicitly creates basis functions that vary on that scale to use in the coarse-scale discretization. These functions are constructed by solving local fine-scale problems with boundary conditions especially chosen to form coarse-scale nodal basis functions. In this study, we used the oscillatory boundary conditions discussed in [*Hou and Wu*, 1997, Section 2.2], as our tests with the alternative (and more expensive) technique of oversampling did not yield any gain in accuracy for these problems. The long correlation lengths considered here suggest a strategy of oversampling to the global scale; while this may be effective for multiphase or time-dependent problems, for the single-phase, steady-state problems considered here, the added cost cannot be appropriately amortized.

To compare the accuracy and efficiency of MLUPS and MSFEM we consider mean uniform flow through this sequence of highly heterogeneous conductivity fields. Specifically, no-flow boundary conditions are applied on the top ($y = 1$) and bottom ($y = 0$), while the hydraulic head is prescribed on the left and right edges, with $h(0, y) = 1$ and $h(1, y) = 0$. In all cases, the computational fine-scale discretization used the standard bilinear Galerkin Finite Element discretization (BLFEM) outlined in Section 2. For both MLUPS and MSFEM we used a computational fine-scale mesh of 256×256 and coarsened (upscaled) by a factor of 32 to an 8×8 mesh. An over-resolved calculation on a 2048×2048 element mesh is used to represent the true solution of this problem, and the BLFEM, MLUPS, and MSFEM solutions are defined at the nodes of this mesh through their basis function representations.

First, we highlight important qualitative differences observed in the MLUPS and MSFEM computations of fine-scale hydraulic head in the neighborhood of coarse-scale element edges. Consider the cross-sections of the hydraulic head that are shown in Figure 7, for the case of the 30° axis

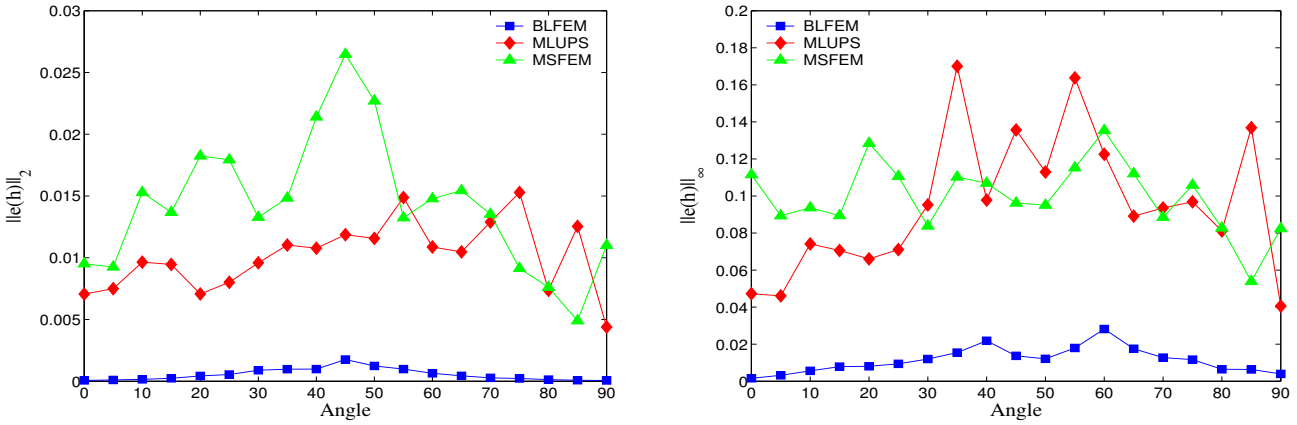

Figure 8. $L_2([0,1]^2)$ (left) and L_∞ errors in the hydraulic head for different angles of the principle axis. Note that the magnitudes of these errors are comparable for both MLUPS and MSFEM and are both significantly larger than that of the BLFEM solution to the 256×256 mesh problem.

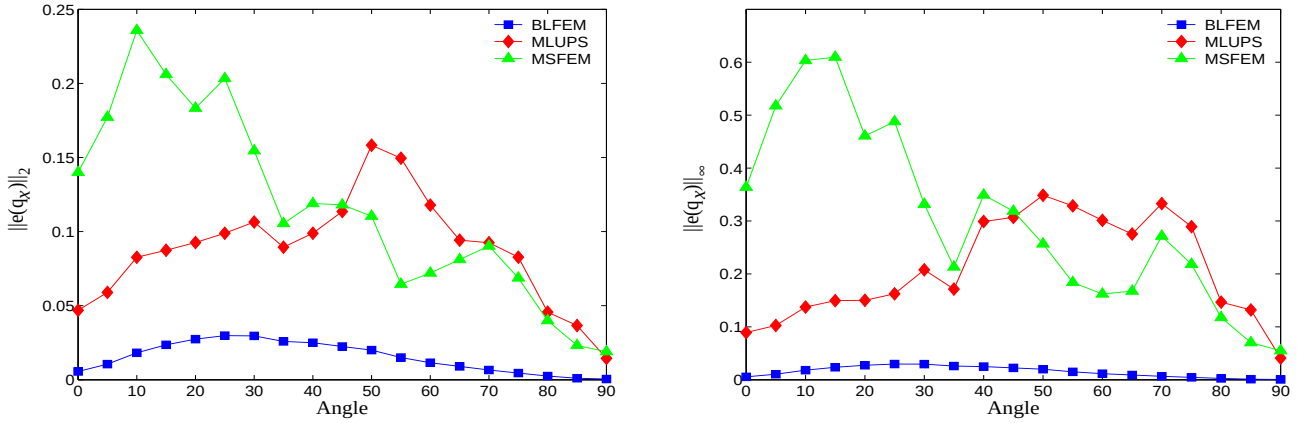

Figure 9. $L_2([0,1])$ error (left) and L_∞ error (right) in the average normal flux for different angles of the principle axis.

of anisotropy field (as in Figure 5). While both upscaled solutions deviate from the fine scale, the MLUPS solution appears to better match the desired behavior. In particular, the MSFEM solution exhibits unnatural abrupt deviations from the fine-scale solution induced by the imposed internal boundary conditions (seen, for example, in the left of Figure 7, around $x = \frac{3}{4}$ and $x = \frac{7}{8}$), while the MLUPS solution has much less dramatic deviations and better matches a number of the features of the fine-scale solution. We note that the BLFEM solution on a 256×256 mesh is too close to the 2048×2048 mesh solution to differentiate on the scales considered in Figure 7; although there are small differences between the two, as indicated by the global error norms presented in Figure 8.

Next, as in Section 3, we consider measures of error in both the head and average normal flux for uniform mean flow from left to right across the domain. Errors in both the hydraulic head and the average flux are calculated relative to the fine-scale solution, measured using the discrete vector norms defined in Equations (14) through (18). Plots of the errors in hydraulic head for the BLFEM, MLUPS, and MSFEM computations on 5 degree steps of the orientation of the conductivity layers are shown in Figure 8, with the $L_2(\Omega)$ given by Equation (14) on the left, and the $L_\infty(\Omega)$ given by Equation (15) on the right. The errors for the bilinear solution on the 256×256 element grid (BLFEM) are presented here as a baseline for the upscaling methods. In some sense, these represent the best we can expect in the upscaled results, illustrating the error in the solution of the computational fine-scale model.

In these plots, we see that the MLUPS and MSFEM methods produce solutions with errors of similar magnitude for these test problems. The MLUPS technique appears to be slightly more accurate for small angles in the orientation of the conductivity layers, although such a generalization would not be possible without large ensemble averages that

are beyond the scope of this study. For larger angles, the errors of the two methods are comparable, with moderate oscillation in the magnitude of the errors for both techniques.

Plots of the errors in average normal flux, integrated along lines of constant x, are shown in Figure 9. The $L_2([0,1])$ norm of average normal flux is computed according to Equation (17) and is shown on the left, while the $L_\infty([0,1])$ is given by Equation (18) and is shown on the right. Once again, we note that the overall similarity in accuracy between the two methods in these error measures, although we see relatively large excursions in computed fluxes for the MSFEM solution for small angles. In general, significant fluctuation with x in the computed average fluxes was seen with the MSFEM procedure, whereas the MLUPS computations were more consistent. This can be seen in the closer relationship between the L_2 and L_∞ norms of the flux for the MLUPS method.

Given the similar accuracy of these two methods, the MLUPS methodology is much more attractive due to its lower computational cost. Specifically, the MSFEM computation requires three fine-scale solves per coarse-scale element to create a full set of basis functions (*Hou and Wu* [1997]). With the existence of optimal solvers such as multigrid for this class of problems, this setup phase has a cost that is proportional to the cost of solving the computational fine-scale system. In fact, using BoxMG (*Dendy* [1982]) to solve the 256×256 element computational fine-scale problems, solution time ranges from approximately 1 to 2.5 seconds on a system with a 1.6 GHz Athlon processor. This variation in solution time is due to the variations in the realizations of the conductivity across different angles, resulting in a degradation in the smoothing rate for some configurations and, hence, a degradation in the convergence of BoxMG. The corresponding MSFEM calculations for upscaling to an 8×8 coarse computational-scale mesh consistently required 1.8 seconds of CPU time on the same machine. In contrast, the MLUPS calculation consistently needed only 0.12 seconds of CPU time, a factor of 15 faster than the MSFEM computation. The dominant cost in each approach is the computation of the basis functions and coarse-scale models. In MLUPS, the cost of computing the interpolation operators (and thus, the basis functions) is quite small, and the cost of computing the coarse-scale operators is roughly the same as the cost of two relaxation sweeps on the finer scale. Thus the setup cost for MLUPS is approximately that of a single V(1,1) cycle. In contrast, for the MSFEM basis functions, typically 5 multigrid V(1,1)-cycles were needed to compute each of the basis functions over their non-zero support. As three basis functions need to be computed over each element (the fourth is given by the requirement of a conforming method) and each basis function computation is 5 times more expensive than the MLUPS computation (as 5 cycles are required with 2 relaxations on each level), we see that the observed factor of 15 times speedup from MSFEM to MLUPS is consistent with the differences in the algorithms. Because the computation of the individual basis functions for MSFEM and the computational coarse grids were so small, the MSFEM and MLUPS approaches did not see the same fluctuation in CPU time as the fine-scale computations did.

5. Conclusions

We demonstrate the capability of the multilevel upscaling methodology to efficiently generate a complete hierarchy of self-consistent coarse-scale models, as well as the corresponding multiscale basis functions, thereby facilitating the computation of coarse- and fine-scale properties of the solution. In this study, our multilevel upscaling algorithm (MLUPS) achieves accuracy comparable to the popular Multiscale Finite Element Method (MSFEM) for computations of both the fine-scale hydraulic head and the average normal flux in strongly heterogeneous media under mean uniform flow. Moreover, the variational coarsening employed in MLUPS provides an efficient means of both computing and representing the multiscale basis functions and, hence, delivers a significant computational savings over MSFEM. In the future, we plan to leverage this natural hierarchical setting to investigate adaptivity and error estimation in both deterministic and stochastic upscaling for more complex flow regimes, such as time-dependent, unsaturated, multiphase, and reactive flows. In addition, we plan to use the solid mathematical framework that this new multilevel upscaling methodology provides to study the apparent scale dependence of various hydrogeologic parameters (cf. *Neuman and Federico* [2003]).

Acknowledgments. The authors would like to thank Xiao-Hui Wu for generously providing the MSFEM code that we used to perform the comparison in this paper. Also, we thank the referees for their insightful and constructive comments. This work was sponsored by the Department of Energy under grant numbers DE-FC02-01ER25479 and DE-FG03-99ER25217, Los Alamos National Laboratory under contract number W-7405-ENG-36, Lawrence Livermore National Laboratory under contract number B533502, Sandia National Laboratory under contract number 15268, and the National Science Foundation under grant numbers DMS-9810751 and DMS-0410318.

References

Bank, R. E., J. Mandel, and S. F. McCormick, Variational multigrid theory, in *Multigrid Methods*, pp. 131–178, SIAM, Philadelphia, 1985.

Braess, D., and W. Hackbusch, A new convergence proof

for the multigrid method including the V cycle, *SIAM J. Numer. Anal.*, *20*, 967–975, 1983.

Brandt, A., *Multigrid Techniques: 1984 Guide with Applications to Fluid Dynamics*, The Weizmann Institute of Applied Science, Rehovot, Israel, 1984.

Briggs, W. L., V. E. Henson, and S. F. McCormick, *A Multigrid Tutorial*, SIAM Books, Philadelphia, 2000, second edition.

Cardwell, W., and R. Parsons, Average permeabilities of heterogeneous oil sands, *Trans. Am. Inst. Min. Metall. Pet. Eng.*, *160*, 34–42, 1945.

Dendy, J. E., Black box multigrid, *J. Comput. Phys.*, *48*, 366–386, 1982.

Desbarats, A. J., Spatial averaging of hydraulic conductivity in 3-dimensional hetergenous porous-media, *Mathematical Geology*, *24*, 249–267, 1992a.

Desbarats, A. J., Spatial averaging of transmissivity in heterogeneous fields with flow toward a well, *Water Resour. Res.*, *28*, 757–767, 1992b.

Deutsch, C., and A. Journel, *GSLIB, geostatistical software library and user's guide*, second ed., Oxford University Press, Oxford, 1998.

Durlofsky, L. J., Numerical-calculation of equivalent grid block permeability tensors for heterogeneous porous-media, *Water Resour. Res.*, *27*, 669–708, 1991.

Ebrahimi, F., and M. Sahimi, Multiresolution wavelet coarsening and analysis of transport in heterogeneous media., *Physica A*, *316*, 160 – 88, 2002.

Grauschopf, T., M. Griebel, and H. Regler, Additive multilevel-preconditioners based on bilinear interpolation, matrix dependent geometric coarsening and algebraic multigrid coarsening for second order elliptic PDEs, *Appl. Numer. Math.*, *23*, 63–96, 1997.

He, C., M. Edwards, and L. Durlofsky, Numerical calculation of equivalent cell permeability tensors for general quadrilateral control volumes, *Computational Geosciences*, *6*, 29–47, 2002.

Hou, T., and X. Wu, A multiscale finite element method for elliptic problems in composite materials and porous media, *J. Comput. Phys.*, *134*, 169–189, 1997.

Hou, T., X. Wu, and Z. Cai, Convergence of a multiscale finite element method for elliptic problems with rapidly oscillating coefficients, *Math. Comp.*, *68*, 913–943, 1999.

MacLachlan, S., Improving robustness in multiscale methods, Ph.D. thesis, Univerity of Colorado at Boulder, Boulder, Colorado, 2004.

Moulton, J. D., J. E. Dendy, and J. M. Hyman, The black box multigrid numerical homogenization algorithm, *J. Comput. Phys.*, *141*, 1–29, 1998.

Neuman, S. P., and V. D. Federico, Multifaceted nature of hydrogeologic scaling and its interpretation, *Rev. Geophys.*, *41*, 1014 –, 2003.

Nicolaides, R. A., On some theoretical and practical aspects of multigrid methods, *Math. Comp.*, *33*, 933–952, 1979.

Warren, J., and H. Price, Flow in heterogeneous porous media, *Society of Petroleum Engineering Journal*, *1*, 153–169, 1961.

Wen, X.-H., and J. J. Gómez-Hernández, Upscaling hydraulic conductivities in heterogeneous media: An overview, *Journal of Hydrology*, *183*, ix–xxii, 1996.

Ye, S., Y. Xue, and C. Xie, Application of the multiscale finite element method to flow in heterogeneous porous media, *Water Resources Research*, *40*, 2004.

S. P. MacLachlan, Department of Applied Mathematics, University of Colorado, UCB 526, Boulder, CO, 80309-0526, USA. (Scott.MacLachlan@colorado.edu)

J. D. Moulton, Mathematical Modeling and Analysis Group, Los Alamos National Laboratory, Los Alamos, NM 87545, USA. (moulton@lanl.gov)

This preprint was prepared with AGU's LaTeX macros v5.01, with the extension package 'AGU++' by P. W. Daly, version 1.6b from 1999/08/19.